PUBLISHED VERSION

Synthetic aperture microwave imaging with active probing for fusion plasma diagnostics

Shevchenko V F, Freethy S J, Huang B K, Vann R G L

© 2014 UNITED KINGDOM ATOMIC ENERGY AUTHORITY

This article may be downloaded for personal use only. Any other use requires prior permission of the author and the American Institute of Physics. The following article appeared in Fusion Reactor Diagnostics: Proceedings of the International Conference, 9-13 September 2013, Villa Monastero, Varenna, Italy. AIP Conf. Proc. 1612 , 53 (2014) and may be found at : http://dx.doi.org/10.1063/1.4894024

AIP Proceedings

Synthetic aperture microwave imaging with active probing for fusion plasma diagnostics

Vladimir F. Shevchenko, Simon J. Freethy, Billy K. Huang, and Roddy G. L. Vann

Citation: AIP Conference Proceedings **1612**, 53 (2014); doi: 10.1063/1.4894024
View online: http://dx.doi.org/10.1063/1.4894024
View Table of Contents: http://scitation.aip.org/content/aip/proceeding/aipcp/1612?ver=pdfcov
Published by the AIP Publishing

Articles you may be interested in

Recent advancements in microwave imaging plasma diagnostics
Rev. Sci. Instrum. **74**, 4239 (2003); 10.1063/1.1610781

Synthetic aperture ultrasound imaging system
J. Acoust. Soc. Am. **96**, 3837 (1994); 10.1121/1.410511

Active synthetic aperture sonar: The past 25 Years
J. Acoust. Soc. Am. **95**, 2950 (1994); 10.1121/1.409072

Synthetic aperture active underwater imaging system
J. Acoust. Soc. Am. **92**, 625 (1992); 10.1121/1.404081

Plasma diagnostics with computerimaged microwave holography
J. Appl. Phys. **53**, 4122 (1982); 10.1063/1.331234

This article is copyrighted as indicated in the article. Reuse of AIP content is subject to the terms at: http://scitation.aip.org/termsconditions. Downloaded to IP: 194.81.223.66 On: Mon, 15 Sep 2014 14:10:26

Synthetic Aperture Microwave Imaging with Active Probing for Fusion Plasma Diagnostics

Vladimir F. Shevchenko[a], Simon J. Freethy[a], Billy K. Huang[a], Roddy G.L. Vann[b]

[a]*EURATOM/CCFE Fusion Association, Culham, Abingdon, Oxon, OX14 3DB, U.K.*
[b]*York Plasma Institute, Dept. of Physics, University of York, York YO10 5DD, U.K.*

Abstract. A Synthetic Aperture Microwave Imaging (SAMI) system has been designed and built to obtain 2-D images at several frequencies from fusion plasmas. SAMI uses a phased array of linearly polarised antennas. The array configuration has been optimised to achieve maximum synthetic aperture beam efficiency. The signals received by antennas are down-converted to the intermediate frequency range and then recorded in a full vector form. Full vector signals allow beam focusing and image reconstruction in both real time and a post-processing mode. SAMI can scan over 16 pre-programmed frequencies in the range of 10-35GHz with a switching time of 300ns. The system operates in 2 different modes simultaneously: both a 'passive' imaging of plasma emission and also an 'active' imaging of the back-scattered signal of the radiation launched by one of the antennas from the same array. This second mode is similar to so-called Doppler backscattering (DBS) reflectometry with 2-D resolution of the propagation velocity of turbulent structures. Both modes of operation show good performance in fusion plasma experiments on Mega Amp Spherical Tokamak (MAST). We have obtained the first ever 2-D images of BXO mode conversion windows. With active probing, first ever turbulence velocity maps have been obtained. We present an overview of the diagnostic and discuss recent results.

In contrast to quasi-optical microwave imaging systems SAMI requires neither big aperture viewing ports nor large 2-D detector arrays to achieve the desired imaging resolution. The number of effective 'pixels' of the synthesized image is proportional to the number of receiving antennas squared. Thus only a small number of optimised antennas is sufficient for the majority of applications. Possible implementation of SAMI on ITER and DEMO is discussed.

Keywords: Nuclear instruments and methods for hot plasma diagnostics; Plasma diagnostics, interferometry, radiometry, spectroscopy and imaging.

PACS: 52.55.Fa, 52.70.-m, 52.25.Os, 47.80.Jk, 07.60.Dq, 07.60.Hv, 52.25.Os, 52.35.Hr, 52.35.Qz.

INTRODUCTION

Microwave and mm-wave radiometry and reflectometry have a very well established reputation in fusion community. Electron cyclotron emission (ECE) radiometry is used for routine electron temperature profile measurements. Reflectometry delivers plasma density profile measurements and it also provides valuable information on density fluctuations and plasma instabilities. Radial resolution in such diagnostics is usually achieved by frequency sweeping or by measurements at several frequencies simultaneously. A complex combination of several types of radiometers and reflectometers are under development for ITER [1]. A strategic advantage of these diagnostics is the possibility of using radiation resilient components. Due to relatively long wavelengths used in these diagnostics, the requirements to the optical systems such as mirrors, antennas and transmission lines are very moderate. Apparently microwave components can withstand even in the DEMO radiation environment [2].

A vast majority of microwave diagnostics developed for fusion experiments including the systems proposed for ITER are essentially one dimensional. Usually measurements can provide radial resolution and sometimes along several viewing chords. Only recently due to advances in microwave technology multi-dimensional measurements become possible [3]. With the multi-dimensional approach the new intriguing physics has been discovered [4]. It was recognized that in ITER several oblique ECE observations should provide information on the electron velocity distribution which may be significantly different from maxwellian in a presence of strong additional heating. Obviously a two dimensional (2D) ECE map resolved in toroidal and poloidal directions would provide even more information on electron distribution and temperature profiles. Major difficulties of using conventional microwave imaging systems in a fusion reactor are related to plasma accessibility requirements. Typically such systems need a big viewing port with a similar size quasi-optical focusing interface and a large 2D detector array located in the nearest proximity which is practically incompatible with neutron shielding requirements.

Fusion Reactor Diagnostics
AIP Conf. Proc. 1612, 53-60 (2014); doi: 10.1063/1.4894024
2014 AIP Publishing LLC 978-0-7354-1248-4/$30.00

This article is copyrighted as indicated in the article. Reuse of AIP content is subject to the terms at: http://scitation.aip.org/termsconditions. Downloaded to IP: 194.81.223.66 On: Mon, 15 Sep 2014 14:10:26

In this paper we propose an alternative imaging system which requires neither big aperture viewing port nor large detector array to achieve required image resolution. It requires a number of individual antennas similar in size to the antennas used for radiometry and/or reflectometry. This system uses an aperture synthesis technique to acquire a 2D map of thermal ECE from the plasma in contrast to photographic imaging used in video-cameras. In synthetic aperture imaging each antenna receives the signals from the whole 2D area within the plasma which needs to be imaged. The ECE signals are recorded in a full vector form (I & Q components) to preserve the phase information within the whole intermediate frequency (IF) bandwidth. Then the image is reconstructed at the post-processing phase by phase manipulation using phased array beam steering technique. Synthetic aperture imaging takes advantage of both ECE radiometry and conventional ECE imaging mentioned above: it delivers 2D images of thermal ECE at several frequencies but it has accessibility requirements similar to a conventional radiometer with all the radiation sensitive components (mixers, local oscillators etc.) located far from the machine.

As an example we discuss the implementation of this technique on Mega Ampere Spherical Tokamak (MAST) [5] at Culham Science Centre, UK. Synthetic Aperture Microwave Imaging (SAMI) system was recently developed and installed on MAST. A detailed description of this diagnostic and some recent results can be found in [6, 7]. Here we focus on the system adaptation to the vacuum interface and discuss its potential as a diagnostic for a fusion reactor.

SAMI ON MAST

SAMI was developed to study thermal emission from over-dense ($\omega_{ce} < \omega_{pe}$) plasma where ω_{ce} is an electron cyclotron frequency and ω_{pe} is a plasma frequency. It is equipped with an array consisting of only n=8 receiving antennas. This array provides n·(n-1)/2 =28 baselines which are equivalent to meaningful pixels in conventional imaging. Relative positioning of the antennas within the array was optimized [8] to achieve best constrains for the reconstructed image. Even with such a limited number of antennas images obtained for the B-X-O mode coupling (MC) windows [9] are sufficiently detailed for comparison with modeling results.

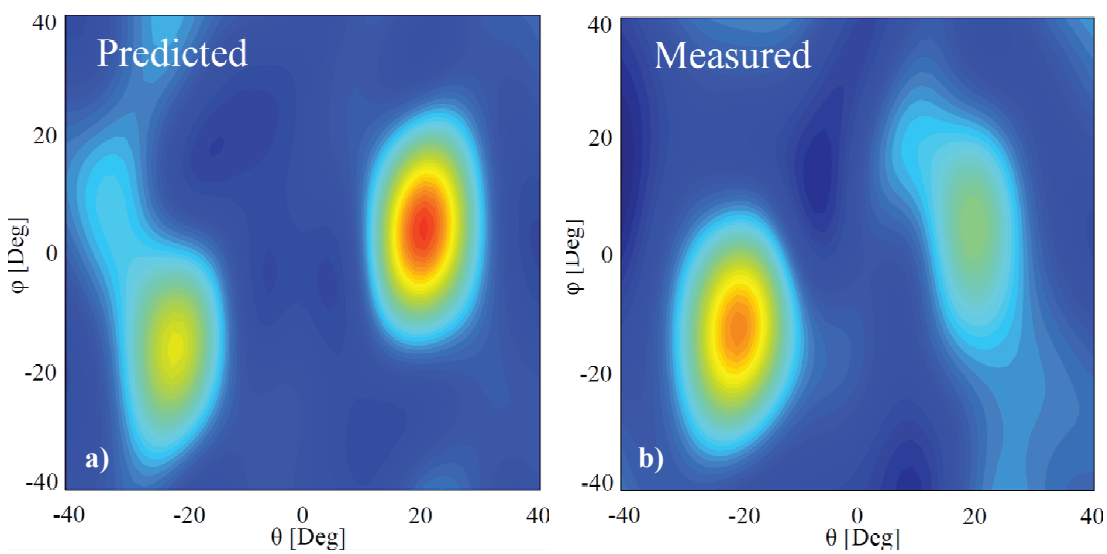

FIGURE 1. a) MC efficiency calculated for 13GHz and convolved with the SAMI point source response from full wave modelling. b) Measured intensity for the shot #27022. Two well-formed and distinct MC windows are clearly seen.

Fig. 1 illustrates the measured thermal ECE from over-dense MAST plasma in comparison with a simulated image for the same plasma parameters. Two distinct maxima are clearly seen in both images. These maxima correspond to the B-X-O MC windows and measured angular coordinates of these windows are in good agreement with simulations. One can see that in simulations the right window appears brighter than the left one while in the measured image the left window appears brighter. This difference can probably be attributed to 2D effects predicted theoretically [10, 11] but not included in our 1D modeling.

This article is copyrighted as indicated in the article. Reuse of AIP content is subject to the terms at: http://scitation.aip.org/termsconditions. Downloaded to IP: 194.81.223.66 On: Mon, 15 Sep 2014 14:10:26

In SAMI, thermal ECE images are recorded sequentially at 16 different local oscillator (LO) frequencies within the range of 10 – 35GHz. This frequency span covers the first 3 EC harmonics in MAST as seen from the low field side of the machine. The LO frequency can be switched every 10μs providing a very fast scan over preprogrammed frequencies [12]. With the existing antenna array ECE images are reconstructed with ±40 degree angular coverage both toroidally and poloidally. For each frequency SAMI produces two images corresponding to the lower side band (LSB) and the upper side band (USB). Side band separation is performed numerically at the post-processing stage. Signals are digitized at the rate of 250 mega-samples per second. The digitization rate defines the intermediate frequency (IF) bandwidth in SAMI. Thus LSB and USB images are integrated over 125MHz IF bandwidth on both sides of the LO frequency. Usually in tokamaks different EC frequencies correspond to different radial origins of ECE providing radial resolution of imaging in addition to 2D angular mapping. A combination of largely separated LO frequencies ~1GHz with closely positioned side band frequencies give an opportunity to study fast radially varying effects together with slow variations over the radius.

Ideally thermal ECE must be recorded at two orthogonal polarizations simultaneously. In this case exact reconstruction of ECE polarization is possible allowing simplified separation of plasma emission from stray radiation bouncing with the vacuum vessel. At present a limited number of receiving channels restricts polarization measurements on MAST but we plan to conduct such experiments in the future.

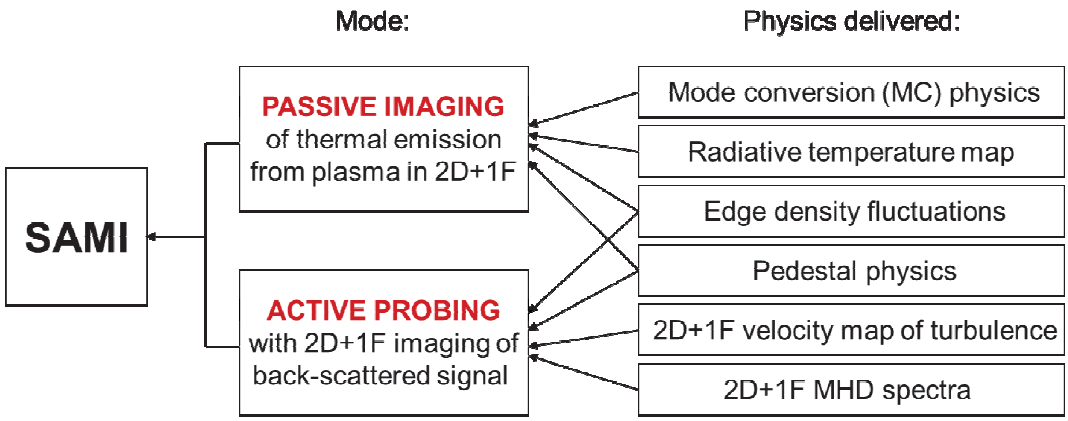

FIGURE 2. Physics delivered by SAMI operating in 2 modes simultaneously.

In addition to the main mode of operation, acquiring passive 2D+1F images of thermal emission from the plasma, SAMI can simultaneously do 2D+1F imaging of back-scattered signals with active probing of plasma. This mode of operation takes advantage of the relatively wide IF bandwidth. The probing signal is generated from LO signal by introducing a several MHz frequency up- or down-shift. There are 3 frequencies 8, 10 and 12MHz available in SAMI to produces up to 3 probing signals simultaneously. A separate antenna or antennas are used to illuminate the plasma with probing beams. Monochromatic parts of the reflected signals are then notched out while frequency shifted signals are extracted in order to analyse induced Doppler shifts due to plasma flows. Simultaneous probing with 2 or 3 beams increases the accuracy and reliability of the reconstructed velocity map. Active probing does not affect thermal ECE imaging because only a small fraction of the available IF bandwidth from 7 to 13MHz is used for the analysis of back-scattered signals. Fig. 2 illustrates a variety of physics accessible with SAMI operation with active probing. Preliminary experimental results obtained with this diagnostics on MAST are discussed in [7].

VACUUM INTERFACE

An important part of the implementation of such a system in a real fusion experimental set-up is inclusion of the vacuum interface into the data analysis. Calibration of the imaging system can be easily conducted in laboratory conditions using a monochromatic point source or a 2D noise source. However calibration in situ is not always possible while the effects induced by vacuum windows and flanges can cause significant distortions of reconstructed

This article is copyrighted as indicated in the article. Reuse of AIP content is subject to the terms at: http://scitation.aip.org/termsconditions. Downloaded to IP: 194.81.223.66 On: Mon, 15 Sep 2014 14:10:26

images. In this section we describe a method to account for various effects due to the vacuum interface. It is based on a full wave 3D modeling of the antenna array including all components which can affect the image.

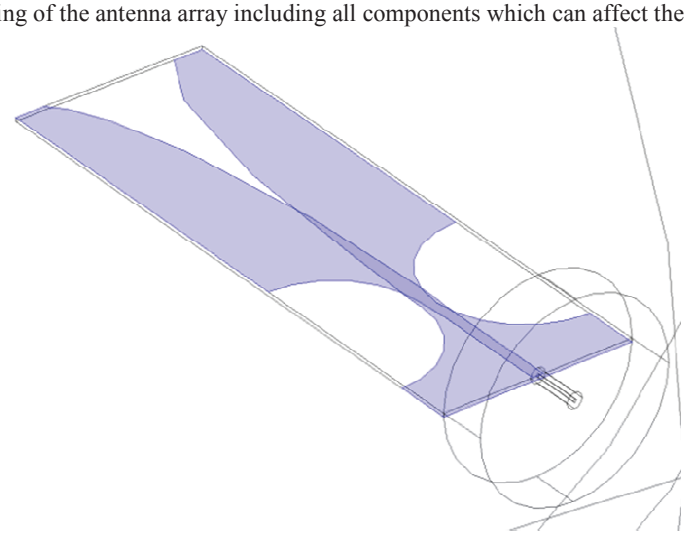

FIGURE 3. 3D model of an antipodal Vivaldi antenna with a 50Ω coaxial feed

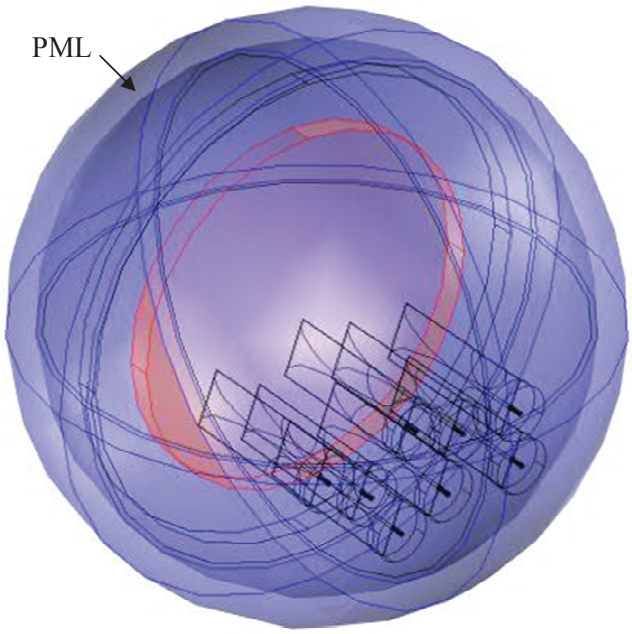

FIGURE 4. Array of Vivaldi antennas with the vacuum interface surrounded by the perfectly matching layer (PML).

First, a realistic model of the antenna must be developed as a building block for the antenna array. In SAMI we use so-called antipodal Vivaldi antennas due to their ultra-broadband performance and a relatively low cost. A CAD design of the antenna including a coaxial feed is shown in Fig. 3. The antenna consists of two conductive (copper) flares etched on opposite sides of PCB board made of 0.381mm thick duroid [6]. One flare is earthed while another is connected to the central conductor of the 50Ω coaxial feed. Then this antenna is surrounded by a spherical perfectly matching layer (PML) which does not provide any reflection for outgoing waves. The antenna is excited with a monochromatic signal. A 3D electromagnetic field map produced by the single antenna is calculated using commercial software package COMSOL allowing full wave 3D simulations. In parallel a real antenna with the same

This article is copyrighted as indicated in the article. Reuse of AIP content is subject to the terms at: http://scitation.aip.org/termsconditions. Downloaded to IP: 194.81.223.66 On: Mon, 15 Sep 2014 14:10:26

geometry was experimentally tested in the lab. The antenna was placed in an anechoic chamber and the directivity diagrams were measured in E and H-planes using a scalar network analyzer. Comparison with simulations showed good agreement providing us with a confidence for the further steps in our modeling.

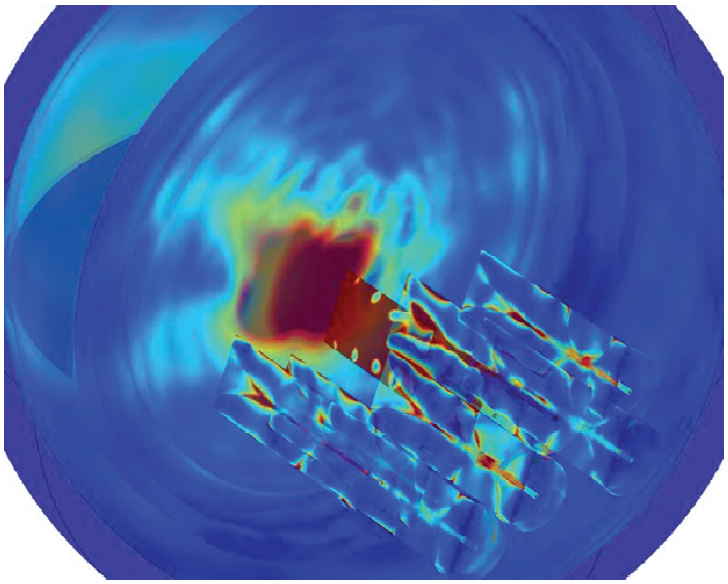

FIGURE 5. Electric field generated by the antenna located near the centre of the array and induced signals in neighbouring antennas.

The antenna array model is built using the above model of the single antenna. The array model includes the vacuum window and stainless steel flange around it exactly reproducing the geometry on the machine. Similar to the case of the single antenna the array with the vacuum interface is surrounded by the spherical PML providing absence of reflection for any outgoing wave (see Fig. 4).

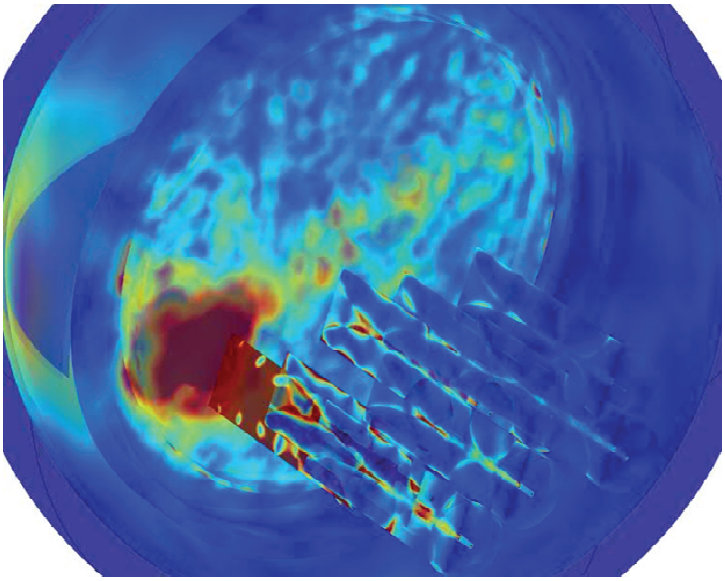

FIGURE 6. Same as in Fig. 5 with the active antenna located at the edge of the array.

This article is copyrighted as indicated in the article. Reuse of AIP content is subject to the terms at: http://scitation.aip.org/termsconditions. Downloaded to IP: 194.81.223.66 On: Mon, 15 Sep 2014 14:10:26

In such a model it is possible to account for the antenna cross-talk effects and interference due to reflections from the window and the flange. To achieve that only one antenna is excited at a time while other antennas are passively terminated by 50Ω loads. Fig. 5 shows a simulated electric field generated by the single antenna #4 located close to the centre of the array. Fig. 6 illustrates the case when the antenna #7 located at the edge of the array was active. One can see a strong and regular interference pattern within the vacuum window in the case of active antenna #4. In the case of active antenna #7 interference is also strong but the pattern doesn't appear regular because reflections from the flange break regular standing waves. This type of interference produces significant distortion of the recorded image. One can also see that every passive antenna receives a non-zero signal due to direct cross-talk between antennas and because of reflections from the window and the flange. Cross-talk and reflection can be separated and analysed individually by repeating simulations without the vacuum interface. However it is important to take account for all these effects simultaneously. Cross-talk is accounted for by creating a matrix of mutual coupling coefficients between individual antennas within the array with further corrections to the experimental signals. Interference is accounted for in the following way. 2D electromagnetic field map generated by every single antenna is calculated at the plane behind the vacuum interface. As an example, such a map for antenna #7 is shown in Fig. 7.

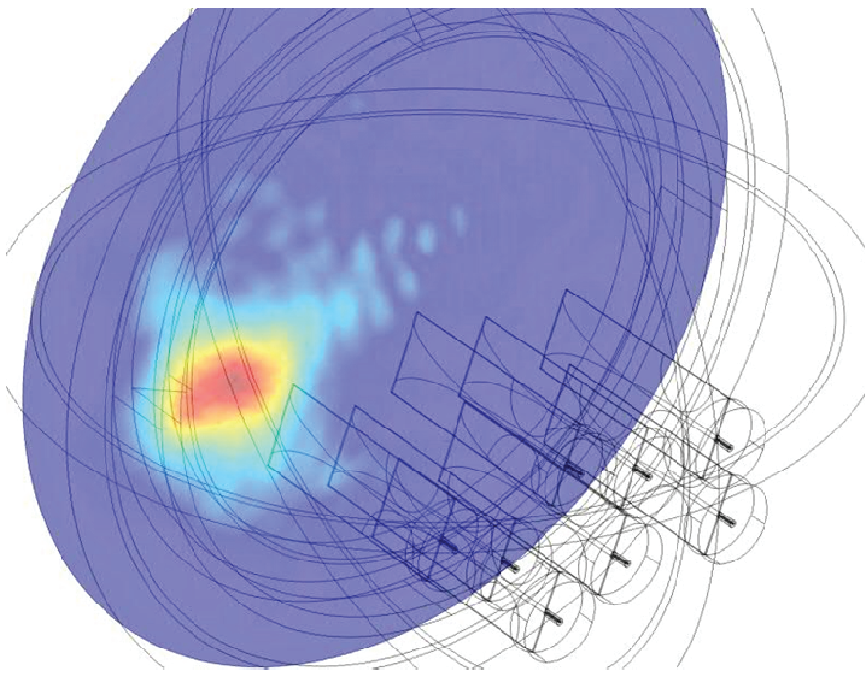

FIGURE 7. Electric field generated by antenna #7 with vacuum window and flange included.

Then this field is analytically extended into the quasi far-field zone [13] corresponding to the emitting plasma surface. This extension is done within the antenna coverage angles. This procedure is repeated for every single antenna and for every LO frequency available. Now we have all necessary information to generate a synthesized beam which is adequate to the signals received by SAMI on MAST. To generate such a beam the analytically extended vector fields from individual antennas are summed with appropriate phasing corresponding to one particular viewing angle. Then constructive interference forms the beam pattern while destructive interference clears up surrounding background. An example of the beam generated in this way for viewing angles of -10 degrees toroidally and of -15 degrees poloidally is shown in Fig. 8. It shows the presence of small side lobs which are unavoidable in beam forming technique. However the relative intensity in the side lobs is much smaller in comparison with the main beam. This beam pattern also includes the effect from the MAST poloidal field coil which is obscuring the viewing angles above 25 degrees in the poloidal direction and producing some reflection from the

This article is copyrighted as indicated in the article. Reuse of AIP content is subject to the terms at: http://scitation.aip.org/termsconditions. Downloaded to IP: 194.81.223.66 On: Mon, 15 Sep 2014 14:10:26

metallic coil case. Thus to account for the effects of the vacuum interface these synthesised beam patterns must be summed for every viewing angle with the weighting factor calculated by the beam forming technique [6].

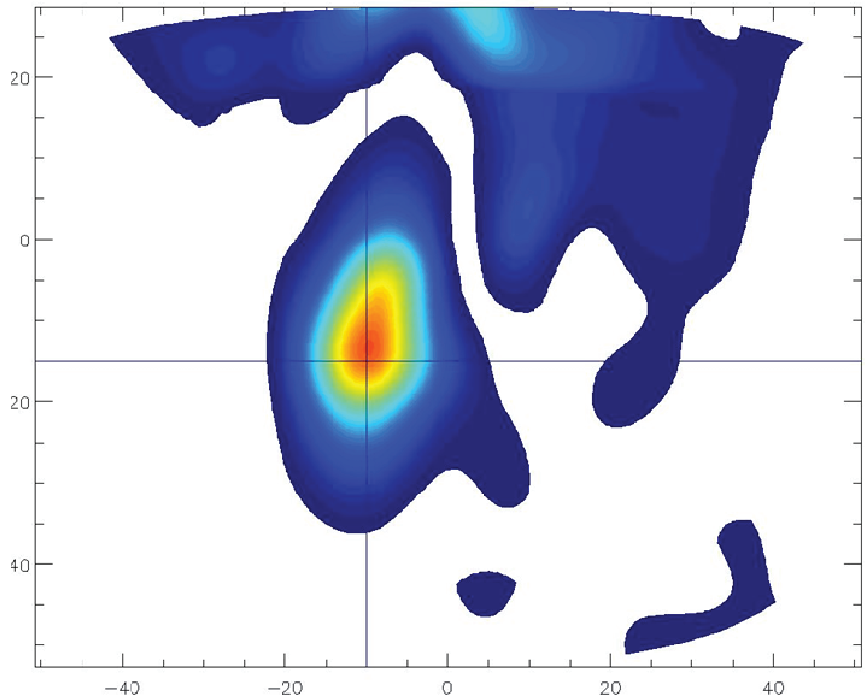

FIGURE 8. Synthesised beam pattern generated by all 8 phased antennas at 13 GHz.

CONCLUSIONS

A microwave imaging system with ~10 μs time resolution has been designed and built for fusion plasma research. The system uses a phased array of antennas instead of focusing optics. The principle is based on the fact that phase differences between antenna pairs steer the viewing direction. Cross-correlations between pairs of antennas give the spatial Fourier transform of the emission pattern. The effective number of "pixels" is ~ N^2 (where N is the number of antennas). A phased array of 8 antennas has been implemented on the MAST tokamak to record the first 2D images of thermal microwave emission escaping from the plasma.

The system records images at 16 discrete frequencies switching in a programmable manner within the range of 10-35 GHz (covering the range from ω_{ce} to $3\cdot\omega_{ce}$). Frequency scanning provides radial resolution in addition to 2D images resulting in 2D+1F(R) resolution over the frequency scan. All signal processing stages including side band separation are performed digitally post-shot. Two images are generated at every frequency corresponding to the lower and upper side bands. Side band separation is about 0.1 GHz. The first ever 2D images of mode converted Bernstein wave emission have been experimentally obtained from a fusion plasma. Experimental 2D images are in good agreement with mode coupling modeling results.

Simultaneously with passive imaging of the thermal emission from the plasma, the system performs active probing of the plasma surface. The probing signal is back-scattered by the plasma turbulence. The frequency of the scattered signal is Doppler shifted due to the turbulent motion. The system acquires scattered signals and produces a 2D velocity map of the plasma turbulence at every probing frequency. That is the first ever 2D turbulence velocity map experimentally measured in fusion plasmas.

MAST synthetic aperture imaging system was considered as an example of implementation of this technique on tokamak. The use of full wave modeling to account for the vacuum interface is described in details. It becomes important in the next generation fusion experiments where calibration in situ is impossible. In contrast to quasi-

This article is copyrighted as indicated in the article. Reuse of AIP content is subject to the terms at: http://scitation.aip.org/termsconditions. Downloaded to IP: 194.81.223.66 On: Mon, 15 Sep 2014 14:10:26

optical microwave imaging systems SAMI requires neither big aperture viewing ports nor large 2-D detector arrays to achieve the desired imaging resolution. It needs only a small number of individual antennas similar in size to the antennas used for radiometry and/or reflectometry. Synthetic aperture imaging takes advantage of both ECE radiometry and conventional ECE imaging: it delivers 2D images of thermal ECE at several frequencies but it has accessibility requirements similar to conventional radiometer with all radiation sensitive components located far from the machine.

ACKNOWLEDGMENTS

This work was funded partly by EPSRC under grant EP/H016732, by the University of York, by the RCUK Energy Programme under grant EP/I501045 and the European Communities under the contract of Association between EURATOM and CCFE. The views and opinions expressed herein do not necessarily reflect those of the European Commission.

REFERENCES

1. A. J. H. Donne et al. *Nucl. Fusion*, **47,** S337–S384, (2007).
2. W. Biel, Plasma diagnostics and control in future magnetic fusion reactors: Requirements and implementation issues, *this conference,* (2013).
3. H. K. Park et al. Recent advancements in microwave imaging plasma diagnostics. *Rev. Sci. Instrum*., **74**(10), (2003).
4. H. K. Park et al. *Phys. Rev. Lett*, **96,** 195004 (2006).
5. A. Darke et al. MAST: a Mega Amp Spherical Tokamak, in the proceedings of the *18th Symposium on Fusion Technology*, August 22–26, Karlsruhe, Germany (1994).
6. V. F. Shevchenko et al. Synthetic aperture microwave imaging with active probing for fusion plasma diagnostics. *Journal of Instrumentation*, JINST **7**, P10016, (2012).
7. S. J. Freethy et al. *Plasma Phys. Control. Fusion*, accepted for publication (2013).
8. S. J. Freethy et al. Optimization of wide field interferometric arrays via simulated annealing of a beam efficiency function. *IEEE Transactions on Antennas and Propagation*, **60**(11), (2012).
9. V. F. Shevchenko et al. Two dimensional studies of electron Bernstein wave emission in MAST. *Fusion Science and Technology*, **59**(4), 663-669, (2011).
10. A. Yu. Popov, *Plasma Phys. Control. Fusion,* **52,** 035008, (2010).
11. E. D. Gospodchikov, T. A. Khusainov and A. G. Shalashov, *Plasma Phys. Control. Fusion,* **54,** 045009, (2012).
12. B. K. Huang et al., FPGA-based embedded Linux technology in fusion: MAST microwave imaging system, *Fusion Engineering and Design*, (2012).
13. S. A. Schelkunoff, *Bell Syst. Tech. J.*, **15**(1), 92, (1936).

This article is copyrighted as indicated in the article. Reuse of AIP content is subject to the terms at: http://scitation.aip.org/termsconditions. Downloaded to IP: 194.81.223.66 On: Mon, 15 Sep 2014 14:10:26